Role of Noether's Theorem at the Deconfined Quantum Critical Point

Nvsen Ma,[1] Yi-Zhuang You,[2,3] and Zi Yang Meng[1,4,5,6]

[1]*Beijing National Laboratory for Condensed Matter Physics and Institute of Physics,*
Chinese Academy of Sciences, Beijing 100190, China
[2]*Department of Physics, University of California, San Diego, California 92093, USA*
[3]*Department of Physics, Harvard University, Cambridge, Massachusetts 02138, USA*
[4]*Department of Physics, The University of Hong Kong, Pokfulam Road, Hong Kong, China*
[5]*CAS Center of Excellence in Topological Quantum Computation and School of Physical Sciences,*
University of Chinese Academy of Sciences, Beijing 100190, China
[6]*Songshan Lake Materials Laboratory, Dongguan, Guangdong 523808, China*

Noether's theorem is one of the fundamental laws of physics, relating continuous symmetries and conserved currents. Here we explore the role of Noether's theorem at the deconfined quantum critical point (DQCP), which is a quantum phase transition beyond the Landau-Ginzburg-Wilson paradigm. It was expected that a larger continuous symmetry could emerge at the DQCP, which, if true, should lead to conserved current at low energy. By identifying the emergent current fluctuation in the spin excitation spectra, we can quantitatively study the current-current correlation in large-scale quantum Monte Carlo simulations. Our results reveal the conservation of the emergent current, as signified by the vanishing anomalous dimension of the current operator, and hence provide supporting evidence for the emergent symmetry at the DQCP. Our study demonstrates an elegant yet practical approach to detect emergent symmetry by probing the spin excitation, which could potentially guide the ongoing experimental search for the DQCP in quantum magnets.

Introduction.—Noether's theorem is a profound theorem in physics that states every continuous (differentiable) symmetry of a physical system is associated with a corresponding conservation law [1]. Well-known examples include momentum and energy conservation, when the system respects space and time translation symmetries. The conservation law usually manifests itself in the form of a conserved current J_μ, which satisfies the equation $\partial^\mu J_\mu = 0$. Likewise, the observation of a conserved current in a physical system usually serves as direct evidence of the associated continuous symmetry.

In this Letter, we introduce an explicit application of Noether's theorem in identifying the emergent continuous symmetry in an exotic quantum phase transition—the deconfined quantum critical point (DQCP) [2–6]. The DQCP describes a direct continuous transition between two phases that spontaneously breaks very different symmetries. In particular, we focus on a type of DQCP which has only recently been identified in quantum Monte Carlo (QMC) simulations [6,7], dubbed the easy-plane DQCP. It is a direct quantum phase transition in a $(2 + 1)$D quantum spin model between the antiferromagnetic *XY* (AFXY) ordered phase and the columnar valence bond solid (VBS) phase. The AFXY (VBS) phase is described by the ordering of a two-component spin order parameter (N_x, N_y) [dimer order parameter (D_x, D_y)], which

spontaneously breaks the in-plane U(1) spin rotation symmetry ($\mathbb{Z}_4$ lattice rotation symmetry). At the transition point, both the spin and dimer order parameters fluctuate strongly but with vanishing expectation values, such that the microscopic $U(1) \times \mathbb{Z}_4$ is restored. Remarkably, it has been suggested that the low-energy critical fluctuations could respect an even larger emergent O(4) symmetry, which corresponds to the full rotation of the combined four-component order parameter (D_x, D_y, N_x, N_y). The emergent O(4) symmetry, if it exists, is a hallmark of the easy-plane DQCP [8–10].

Several methods have been developed to test the emergent symmetry at the DQCP, including comparing the critical exponents in spin and VBS channels [5–7,11–18], plotting the order parameter histograms [5,11,17,19–23], and probing the degenerated correlation spectra of spin-0 and spin-1 excitations [24,25]. But the conserved Noether current that is directly associated with the emergent continuous symmetry [26] has not been measured. In this work, we directly probe the SO(4) current fluctuation at the easy-plane DQCP and verify the current conservation by measuring the scaling dimensions of the current-current correlations.

Based on the field theoretical analysis, which captures the emergent O(4) symmetry of the DQCP, we are able to identify different components of the SO(4) current operator

with the microscopic spin operator at different momenta. We then measure imaginary-time correlation functions of these spin fluctuations at the designated momenta in large-scale QMC simulations to determine the critical scaling of the current operator. The conservation of the Noether current $\partial^\mu J_\mu = 0$ implies that the flux of the current $\int_{\partial\Omega} \epsilon^{\mu\nu\lambda} J_\mu dx_\nu dx_\lambda$ through a close manifold $\partial\Omega$ in the $(2+1)$D spacetime must remain constant. As a result, the conserved current should follow a precise scaling law $J_\mu \sim x^{-2}$ with the scaling dimension pinned at 2, which is an integer instead of a usually fractional critical exponent for generic operators [27]. By a systematic finite size scaling of the numerical data, we are able to make quantitative comparison of the measured scaling dimensions with the field theoretical expectation.

Our results are in strong support of the emergent O(4) symmetry, up to the largest system size $L = 96$. The emergent O(4) symmetry generally points to a continuous transition at the easy-plane DQCP, although we can not rule out the possibility of a symmetry-enhanced first-order transition (plausibly due to a pseudocriticality[8]). Such a possibility was recently reported in Refs. [20,29,30] in several related models. Our attempt of bridging the conserved current correlation from basic laws of physics with large-scale numerical calculation of quantum many-body systems provides a complementary and elegant way of identifying the emergent continuous symmetry at quantum phase transitions (not necessarily continuous), which are becoming ubiquitously present in the new paradigms of quantum matter such as various forms of DQCP [2–6,14,17,19–21,29,31,32], frustrated magnets [22, 33–35], interacting topological phases [14,36–38], and quantum electrodynamic systems [10,35,39]. Our numerical study of the conserved current at an emergent O(4) symmetric DQCP will also guide future spectroscopy experiments, neutron scattering for example, in search of DQCP in candidate materials such as the Shastry-Sutherland lattice compond $SrCu_2(BO_3)_2$ [25].

Model.—The easy-plane DQCP was reported in our previous QMC simulation of the easy-plane J-Q (EPJQ) model [6], which is a spin model on a two-dimensional square lattice, as illustrated in Fig. 1(a). The model is described by the following Hamiltonian:

$$H_{\text{EPJQ}} = -J \sum_{\langle ij \rangle} (P_{ij} + \Delta S_i^z S_j^z) - Q \sum_{\langle ijklmn \rangle} P_{ij} P_{kl} P_{mn}, \quad (1)$$

where $\boldsymbol{S}_i = (S_i^x, S_i^y, S_i^z)$ denotes the spin-1/2 operator on each site i and $P_{ij} = \frac{1}{4} - \boldsymbol{S}_i \cdot \boldsymbol{S}_j$ is the spin-singlet projection operator across the bond $\langle ij \rangle$. The summation of $\langle ijklmn \rangle$ runs over all the six-site clusters containing three parallel bonds $\langle ij \rangle$, $\langle kl \rangle$, $\langle mn \rangle$, as shown in Fig. 1(a), which can be arranged either horizontally or vertically.

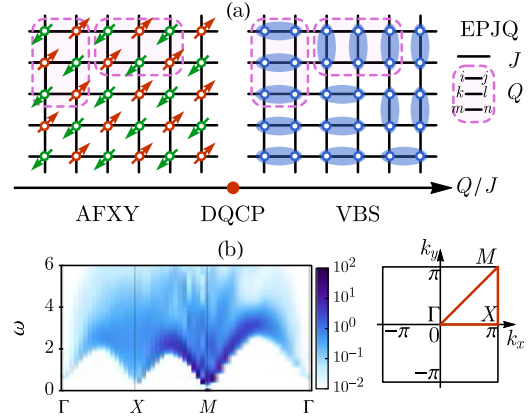The J term describes the nearest neighboring antiferromagnetic ($J > 0$) spin interaction with an easy-plane

FIG. 1. (a) The easy-plane J-Q (EPJQ) model and its phase diagram. The Q term describes the three-dimer interaction in both horizontal and vertical directions, with the arrangement of site indices shown on the right. (b) Obtained spin excitation spectra in the S^x channel of the EPJQ model at the DQCP in our previous work [7]. Darker color indicates higher intensity. The high symmetry points in the Brillouin zone (BZ) are defined on the right.

anisotropy introduced by the $\Delta S_i^z S_j^z$ term ($0 < \Delta \leq 1$). The Q term describes the attractive ($Q > 0$) interaction among three adjacent parallel dimers. The model admits sign-free QMC simulations for all range of parameters. At $\Delta = 0$, the model goes back to the SU(2) symmetric J-Q_3 model [11,40,41]. With finite $\Delta > 0$, the SU(2) spin rotation symmetry is explicitly broken down to its U(1) subgroup, describing the in-plane rotation of XY spins. We define the tuning parameter $q = (Q/J + Q)$ (such that $0 \leq q \leq 1$). When $q \to 0$, the model favors the antiferromagnetic ordered phase of XY spins, denoted as the AFXY phase. When $q \to 1$, the VBS phase is favored. The AFXY and VBS order parameters are defined as

$$N_x = \sum_i (-)^{x_i+y_i} \langle S_i^x \rangle, \qquad D_x = \sum_i (-)^{x_i} \langle P_{i,i+\hat{x}} \rangle, \qquad (2)$$

and N_y, D_y are similarly defined under $x \leftrightarrow y$, where $\boldsymbol{r}_i = (x_i, y_i)$ labels the coordinate of site i on the square lattice and $\hat{x} = (1, 0)$, $\hat{y} = (0, 1)$ are lattice unit vectors. In Ref. [6] it is shown that at $\Delta = 1/2$, the EPJQ model exhibits a direct quantum phase transition between the AFXY and VBS phases at $q_c = (Q/J + Q)_c = 0.62(1)$, realizing the easy-plane DQCP. As argued based on dualities [8,10,42], the critical point is expected to exhibit an emergent O(4) symmetry at low energy, which rotates both the AFXY and VBS order parameters together as an O(4) vector $\boldsymbol{n} = (n^1, n^2, n^3, n^4) = (D_x, D_y, N_x, N_y)$.

Conserved currents.—According to Noether's theorem, the proposed O(4) emergent symmetry at the easy-plane DQCP must be accompanied with the corresponding emergent conserved currents. The goal of this work is to test these emergent conserved currents in numerics. We are interested in the continuous SO(4) subgroup of O(4), which

has six Lie group generators. Each generator A^{ab} is labeled by a pair of ordered indices $a < b$ taken from $a, b = 1, 2, 3, 4$, which generates the rotation between n^a and n^b components of the O(4) vector $\boldsymbol{n}$. If the O(4) symmetry indeed emerges at low energy, we should be able to observe six conserved currents J_μ^{ab}, each corresponds to a generator A^{ab} with three space-time components labeled by $\mu = 0, 1, 2$ (the temporal component is the conserved charge density). By a simple counting, there are $6 \times 3 = 18$ components of the SO(4) conserved currents J_μ^{ab} (6 from ab and 3 from μ indices). Their low-energy and long-wavelength fluctuations are expected to appear as quantum critical fluctuations at the DQCP.

However we do not aim to observe all of the 18 components of J_μ^{ab} here, instead, we will focus on those that are detectable in the *spin* excitation spectrum, which are simpler to measure in QMC simulations (compared to the dimer excitations) and are more relevant to scattering experiments. It was found in Ref. [7] that at the critical point, the spin excitation spectrum will become gapless at four momentum points $\boldsymbol{Q}$: $(0,0)$, $(\pi, 0)$, $(0, \pi)$, and (π, π), as shown in Fig. 1(b) for the S^x channel (the S^z channel shares a similar shape). We will label these low-energy fluctuations by

$$S_{\boldsymbol{Q}}(q) = \sum_i \boldsymbol{S}_i(\tau) e^{iq_0\tau - i(\boldsymbol{Q}+\boldsymbol{q})\cdot\boldsymbol{r}_i}, \qquad (3)$$

where $\boldsymbol{S}_i(\tau)$ is the spin operator on site i at imaginary time τ and $q = (q_0, \boldsymbol{q})$ labels the imaginary frequency and momentum. It turns out that 5 of the 18 components of J_μ^{ab} appear in the spin excitation spectrum, as summarized in Table I. These identifications are made by resorting to the field theory description [26,43,44] of the easy-plane DQCP. The detailed derivations are provided in Sec. I of the Supplemental Material (SM) [45].

The first four currents J_2^{23}, J_1^{13}, J_2^{24}, J_1^{14} are associated with the emergent rotational symmetry between AFXY and VBS order parameters [7]. There is no such symmetry at the lattice level, as is evident from the distinct forms of the order parameters in Eq. (2). The emergent AFXY-VBS rotation symmetry is the most crucial part of the O(4) symmetry group that glues the microscopic U(1) and $\mathbb{Z}_4$ symmetries together. The observation of the conservation

TABLE I. Identification between low-energy spin excitations and emergent SO(4) conserved currents.

Spin	$\boldsymbol{Q}$	Current	Related symmetry
S^x	$(\pi, 0)$	J_2^{23}	(D_y, N_x) rotation
S^x	$(0, \pi)$	J_1^{13}	(D_x, N_x) rotation
S^y	$(\pi, 0)$	J_2^{24}	(D_y, N_y) rotation
S^y	$(0, \pi)$	J_1^{14}	(D_x, N_y) rotation
S^z	$(0,0)$	J_0^{34}	(N_x, N_y) rotation

law for these currents will provide direct evidence for the emergent O(4) symmetry. Given that the above four currents are related by the microscopic $U(1) \times \mathbb{Z}_4$ symmetry, it is sufficient to only focus on J_2^{23}, which corresponds to the $S_{(\pi,0)}^x$ spin fluctuation. By measuring whether $S_{(\pi,0)}^x$ has a vanishing anomalous dimension, we can determine whether J_2^{23} is conserved or not. For comparison, we also study the last (microscopic) conserved current J_0^{34} in Table I, in association with the microscopic U(1) symmetry, which appears as the $S_{(0,0)}^z$ spin fluctuation.

Numerical results.—Suppose the easy-plane DQCP has the proposed O(4) emergent symmetry, this will put a strong constraint on the correlation function of current operators and the consequence can be tested in our QMC simulation. For an emergent conserved current J_μ^{ab}, its correlation function will be universally given by

$$\langle J_\mu^{ab} J_\nu^{ab} \rangle \sim |q| \left(\delta_{\mu\nu} - \frac{q_\mu q_\nu}{|q|^2} \right), \qquad (a, b = 1, 2, 3, 4), \quad (4)$$

which will not receive corrections from gauge fluctuations and spinon interactions. Using the operator correspondence in Table I, the current-current correlation in the field theory can be translated to the spin-spin correlation in the lattice model as

$$\langle S_{(\pi,0)}^x S_{(\pi,0)}^x \rangle \sim \langle J_2^{23} J_2^{23} \rangle \sim (q_0^2 + q_1^2)/|q|^{1-\eta_{(\pi,0)}^x},$$
$$\langle S_{(0,0)}^z S_{(0,0)}^z \rangle \sim \langle J_0^{34} J_0^{34} \rangle \sim (q_1^2 + q_2^2)/|q|^{1-\eta_{(0,0)}^z}. \quad (5)$$

We have introduced two anomalous exponents $\eta_{(\pi,0)}^x$ and $\eta_{(0,0)}^z$ for general consideration. They will vanish separately if their corresponding currents are indeed conserved. In particular, the vanishing $\eta_{(\pi,0)}^x$ will be nontrivial, as it corresponds to the conservation of the emergent current J_2^{23} of AFXY-VBS rotation, which is not expected at the microscopic level. In this way, we can determine the emergent symmetry from the vanishing anomalous exponent of the Noether current. Only a single exponent is needed in this approach. This is different from measuring the nonvanishing anomalous exponents of the order parameters in previous works for O(4) [6,19,39] and SO(5) [5,11,13,15,41] cases, where one needs to compare exponents of different order parameters to determine the emergent symmetry. The conserved current correlation offers an independent probe of emergent continuous symmetry, which is complementary to previous approaches such as the order parameter histogram [5,17,21].

In QMC simulations, the spin-spin correlation $G_{\boldsymbol{Q}}^a(\tau,\boldsymbol{q}) \equiv \sum_{ij} \langle S_i^a(\tau) S_j^a(0) \rangle e^{i(\boldsymbol{Q}+\boldsymbol{q})\cdot(\boldsymbol{r}_i-\boldsymbol{r}_j)}$ (for $a = x, y, z$) can be directly measured in the imaginary time domain and the momentum space. In order to make a comparison with the numerics, we need to Fourier transform the previous field
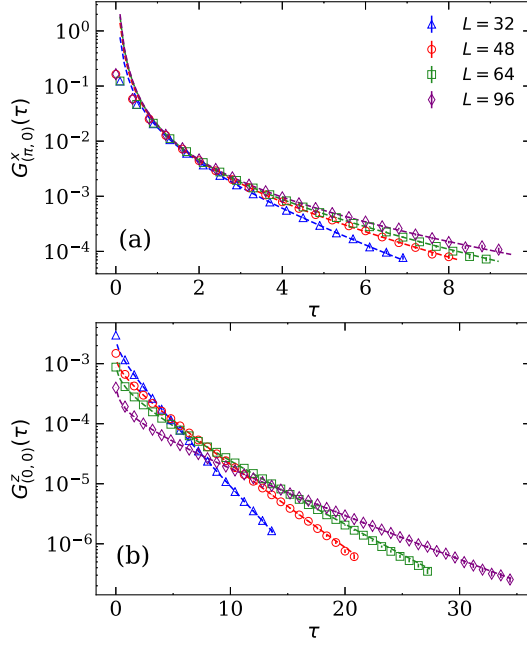
FIG. 2. Spin-spin correlation functions measured at the DQCP of the model in Eq. (1), $q_c = 0.62$, with inverse temperature $\beta = 2L$ and $L = 32, 48, 64, 96$. (a) $G^x_{(\pi,0)}(\tau, \boldsymbol{q})$ and (b) $G^z_{(0,0)}(\tau, \boldsymbol{q})$. All curves in the figures are fitting results using Eq. (6).

theory predictions in Eq. (5) from Matsubara frequency to imaginary time, following $G^a_{\boldsymbol{Q}}(\tau, \boldsymbol{q}) = \int dq_0 e^{-iq_0\tau} \times \langle S^a_{\boldsymbol{Q}}(-q) S^a_{\boldsymbol{Q}}(q) \rangle$. The results are

$$G^x_{(\pi,0)}(\tau, \boldsymbol{q}) \propto q_2^2 F_{\frac{\eta}{2}}(\tau, \boldsymbol{q}) + \frac{\eta+1}{2} F_{\frac{\eta}{2}+1}(\tau, \boldsymbol{q})|_{\eta = \eta^x_{(\pi,0)}},$$

$$G^z_{(0,0)}(\tau, \boldsymbol{q}) \propto \boldsymbol{q}^2 F_{\frac{\eta}{2}}(\tau, \boldsymbol{q})|_{\eta = \eta^z_{(0,0)}}, \tag{6}$$

where $F_\alpha(\tau, \boldsymbol{q}) = |2\boldsymbol{q}/\tau|^\alpha K_\alpha(|\boldsymbol{q}\tau|)$ and $K_\alpha(|\boldsymbol{q}\tau|)$ is the αth order Bessel K function (detailed derivations of Eq. (6) are given in Sec. II of the SM [45]). The anomalous dimensions $\eta^x_{(\pi,0)}$ and $\eta^z_{(0,0)}$ are fitting parameters to be determined from the data. The numerical determination of these exponents from finite size QMC results will be the focus of the narrative below.

Figures 2(a) and 2(b) depict the imaginary time correlations $G^x_{(\pi,0)}(\tau, \boldsymbol{q} = 0)$ and $G^z_{(0,0)}(\tau, \boldsymbol{q})$, respectively. We note that around $\boldsymbol{Q} = (\pi, 0)$, the spin-spin correlation remains finite, so we take the QMC measurements at $(\pi, 0)$; whereas around $\boldsymbol{Q} = (0, 0)$ the spin-spin correlation vanishes with $\boldsymbol{q}$, so we take QMC measurements at a small momentum deviation $2\pi/L$ away from $(0,0)$. Nevertheless, the momentum deviation $\boldsymbol{q}$ in the fitting formula Eq. (6) is still treated as a fitting parameter (of the order $\sim(2\pi/L)$) to partially take care of the finite-size effect. One can see that for the system sizes considered, $L = 32, 48, 64$, and 96 (the others are not shown), the Bessel functions in Eq. (6) fit the data well. In Figs. 2(a) and 2(b), we fit the imaginary time
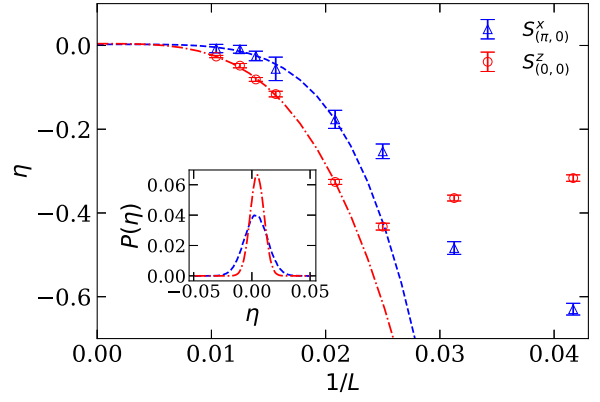

FIG. 3. The anomalous scaling dimensions $\eta^z_{(0,0)}$ and $\eta^x_{(\pi,0)}$ obtained from the fitting in Fig. 2. As L increases, both $\eta^z_{(0,0)}$ and $\eta^x_{(\pi,0)}$ extrapolate to 0, consistent with the prediction of the conserved currents in these two channels. Inset shows the histogram of the extrapolated η obtained from many Gaussian noise realizations of the finite size η values. The histogram of both $\eta^z_{(0,0)}$ and $\eta^x_{(\pi,0)}$ is centered at zero.

data with $\eta^x_{(\pi,0)}$ and $\eta^z_{(0,0)}$ as free fitting parameters. Because the short (imaginary-)time data contain significant contributions from high energy excitations, for which the fitting function is no longer valid, we dynamically choose the fitting range starting from an appropriate short-time cutoff such that $\chi^2/\text{d.o.f.}$ of the fitting is close to one. After fitting all system sizes from $L = 16$ to $L = 96$, the scaling dimensions $\eta^x_{(\pi,0)}$ and $\eta^z_{(0,0)}$ are obtained, and their finite size scalings are given in Fig. 3.

The extrapolated values of the fitted scaling dimensions converge to zero for infinite size within numerical errors as shown in Fig. 3. With the system size up to $L = 96$ we obtain $\eta^x_{(\pi,0)} = 0.002(9)$ and $\eta^z_{(0,0)} = 0.004(6)$ indicating
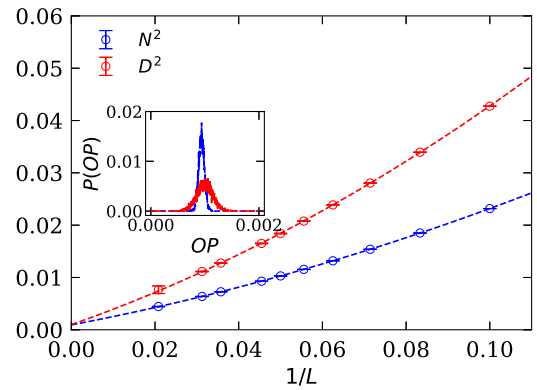

FIG. 4. The finite size extrapolation of the AFXY and VBS order parameters at the easy-plane DQCP. The critical points q_c for each finite size L are determined from their corresponding Binder ratio crossings, and the largest system size is $L = 96$. Inset shows the histogram of extrapolated $\langle N^2 \rangle = 0.0009(2)$ and $\langle D^2 \rangle = 0.0010(3)$.

that the currents J_2^{15} and J_0^{12} are conserved. The conservation of J_0^{12} is just the consequence of spin $U(1)$ symmetry, but the conservation of J_2^{15} is a remarkable observation in favor of the emergent O(4) symmetry at the easy-plane DQCP.

Discussions.—Lastly, let's discuss the extrapolation of the order parameters at the DQCP. As shown in Fig. 4, the AFXY and VBS order parameters $\langle \boldsymbol{N}^2 \rangle = \frac{1}{2}(\langle N_x^2 + N_y^2 \rangle)$ and $\langle \boldsymbol{D}^2 \rangle = \frac{1}{2}(\langle D_x^2 + D_y^2 \rangle)$ are measured for various system sizes at their corresponding finite size $q_c(L)$ [the determination of $q_c(L)$ is discussed in Sec. III of the SM [45]], and with system size up to $L = 96$, the $1/L$ extrapolation gives very small (if not zero) $\langle \boldsymbol{N}^2 \rangle = 0.0009(2)$ and $\langle \boldsymbol{D}^2 \rangle = 0.0010(3)$ at the thermodynamic limit. So at this point, it is possible that the easy-plane DQCP is similar to the recently found symmetry-enhanced first-order transitions [20,29], but with even weaker orders. It is also possible that both order parameters eventually flow to zero, consistent with the original DQCP scenario, i.e., a continuous transition. We leave this to future studies.

To conclude, we have successfully demonstrated Noether's theorem in action in the frontier research of quantum matter—to identify the emergent SO(4) continuous symmetry at easy-plane DQCP. Our attempt stands out as a new numerical tool in identifying emergent continuous symmetry, ubiquitously present at novel quantum phase transitions in DQCP, frustrated magnets, interacting topological phases, and quantum electrodynamic systems. Comparing with the analyses of order parameter histogram and critical exponents, our approach provides a complementary view point both in numerical accessibility and theoretical elegance.

[1] E. Noether, Nachr. Ges. Wiss. Goettingen Math.-Phys. Kl. **1918**, 235 (1918).
[2] O. I. Motrunich and A. Vishwanath, Phys. Rev. B **70**, 075104 (2004).
[3] T. Senthil, A. Vishwanath, L. Balents, S. Sachdev, and M. P. A. Fisher, Science **303**, 1490 (2004).
[4] T. Senthil, L. Balents, S. Sachdev, A. Vishwanath, and M. P. A. Fisher, Phys. Rev. B **70**, 144407 (2004).
[5] A. W. Sandvik, Phys. Rev. Lett. **98**, 227202 (2007).
[6] Y. Q. Qin, Y.-Y. He, Y.-Z. You, Z.-Y. Lu, A. Sen, A. W. Sandvik, C. Xu, and Z. Y. Meng, Phys. Rev. X **7**, 031052 (2017).
[7] N. Ma, G.-Y. Sun, Y.-Z. You, C. Xu, A. Vishwanath, A. W. Sandvik, and Z. Y. Meng, Phys. Rev. B **98**, 174421 (2018).
[8] C. Wang, A. Nahum, M. A. Metlitski, C. Xu, and T. Senthil, Phys. Rev. X **7**, 031051 (2017).
[9] M. A. Metlitski and R. Thorngren, Phys. Rev. B **98**, 085140 (2018).
[10] T. Senthil, D. Thanh Son, C. Wang, and C. Xu, arXiv: 1810.05174.
[11] J. Lou, A. W. Sandvik, and N. Kawashima, Phys. Rev. B **80**, 180414(R) (2009).
[12] M. S. Block, R. G. Melko, and R. K. Kaul, Phys. Rev. Lett. **111**, 137202 (2013).
[13] H. Shao, W. Guo, and A. W. Sandvik, Science **352**, 213 (2016).
[14] Y. Liu, Z. Wang, T. Sato, M. Hohenadler, C. Wang, W. Guo, and F. F. Assaad, arXiv:1811.02583.
[15] R. K. Kaul and A. W. Sandvik, Phys. Rev. Lett. **108**, 137201 (2012).
[16] A. Nahum, J. T. Chalker, P. Serna, M. Ortuño, and A. M. Somoza, Phys. Rev. X **5**, 041048 (2015).
[17] A. Nahum, P. Serna, J. T. Chalker, M. Ortuño, and A. M. Somoza, Phys. Rev. Lett. **115**, 267203 (2015).
[18] J. D'Emidio and R. K. Kaul, Phys. Rev. Lett. **118**, 187202 (2017).
[19] X.-F. Zhang, Y.-C. He, S. Eggert, R. Moessner, and F. Pollmann, Phys. Rev. Lett. **120**, 115702 (2018).
[20] B. Zhao, P. Weinberg, and A. W. Sandvik, arXiv:1804 .07115.
[21] T. Sato, M. Hohenadler, and F. F. Assaad, Phys. Rev. Lett. **119**, 197203 (2017).
[22] Y.-C. Wang, Y. Qi, S. Chen, and Z. Y. Meng, Phys. Rev. B **96**, 115160 (2017).
[23] X. Y. Xu, K. T. Law, and P. A. Lee, Phys. Rev. B **98**, 121406 (R) (2018).
[24] L. Wang and A. W. Sandvik, Phys. Rev. Lett. **121**, 107202 (2018).
[25] J. Y. Lee, Y.-Z. You, S. Sachdev, and A. Vishwanath, arXiv:1904.07266.
[26] M. Hermele, T. Senthil, and M. P. A. Fisher, Phys. Rev. B **72**, 104404 (2005).
[27] We note that there are cases for CFT where the leading power laws of three-point (and higher) correlations are not given simply by the scaling dimensions of the lattice operators involved, but complications can happen such that faster decay is observed due to exact cancellations of contributions from the fields and currents under conformal symmetry. This is explicitly shown in the 1D case by Pranay *et al.* in Ref. [28].
[28] P. Patil, E. Katz, and A. W. Sandvik, Phys. Rev. B **98**, 014414 (2018).
[29] P. Serna and A. Nahum, arXiv:1805.03759.
[30] J. Wildeboer, J. D'Emidio, and R. K. Kaul, arXiv:1808.04731.
[31] R. K. Kaul, R. G. Melko, and A. W. Sandvik, Annu. Rev. Condens. Matter Phys. **4**, 179 (2013).

[32] R.-Z. Huang, D.-C. Lu, Y.-Z. You, Z. Y. Meng, and T. Xiang, arXiv:1904.00021.

[33] R. Moessner and S. L. Sondhi, Phys. Rev. B **63,** 224401 (2001).

[34] S. V. Isakov and R. Moessner, Phys. Rev. B **68,** 104409 (2003).

[35] X. Y. Xu, Y. Qi, L. Zhang, F. F. Assaad, C. Xu, and Z. Y. Meng, arXiv:1807.07574.

[36] F. F. Assaad and T. Grover, Phys. Rev. X **6,** 041049 (2016).

[37] S. Gazit, F. F. Assaad, S. Sachdev, A. Vishwanath, and C. Wang, Proc. Natl. Acad. Sci. U.S.A. **115,** E6987 (2018).

[38] Y.-C. Wang, X. Yang, Y. Ran, and Z. Y. Meng, arXiv: 1810.06751.

[39] N. Karthik and R. Narayanan, Phys. Rev. D **96,** 054509 (2017).

[40] A. Sen and A. W. Sandvik, Phys. Rev. B **82,** 174428 (2010).

[41] A. W. Sandvik, Phys. Rev. Lett. **104,** 177201 (2010).

[42] C. Xu and Y.-Z. You, Phys. Rev. B **92,** 220416(R) (2015).

[43] Y. Ran and X.-G. Wen, arXiv:cond-mat/0609620.

[44] Y.-Z. You, Y.-C. He, A. Vishwanath, and C. Xu, Phys. Rev. B **97,** 125112 (2018).

[45] See Supplemental Material at http://link.aps.org/supplemental/10.1103/PhysRevLett.122.175701 for derivations of the correlation functions for conserved currents, details in the form of Bessel functions of current-current correlations in different momenta in Table I, and the finite size scaling of the AF*XY* and VBS order parameters, which includes Refs. [7,46].

[46] N. Ma, P. Weinberg, H. Shao, W. Guo, D.-X. Yao, and A. W. Sandvik, Phys. Rev. Lett. **121,** 117202 (2018).